J|A|C|S COMMUNICATIONS

Published on Web 08/05/2009

Demonstration of Surface-Enhanced Raman Scattering by Tunable, Plasmonic Gallium Nanoparticles

Pae C Wu,*,† Christopher G. Khoury,*,‡ Tong-Ho Kim,† Yang Yang,§ Maria Losurdo,†,|| Giuseppe V. Bianco,|| Tuan Vo-Dinh,‡ April S. Brown,†,‡ and Henry O. Everitt†,§,⊥

Departments of Electrical and Computer Engineering, Biomedical Engineering, and Physics, Duke University, Durham, North Carolina 27708, Institute for Inorganic Methodologies and of Plasmas (IMIP), CNR, 70126 Bari, Italy, and Army Aviation and Missile RD&E Center, Redstone Arsenal, Alabama 35898

Received May 4, 2009; E-mail: pae.wu@duke.edu

Gallium, a standard metal used for optoelectronic devices, represents an alternative plasmonic material with attributes superior to traditional nanostructured silver and gold. Here we present the first demonstration of plasmonic Ga nanoparticles (NPs) as substrates for surface-enhanced Raman scattering (SERS).

The theoretical treatment by Zeman and Schatz[1] revealed the potential of Ga to support strong surface fields. Plasmonic gallium NPs are promising for an array of applications because of their broad plasmon tunability, stability across a wide temperature range, excellent plasmon resiliency when oxidized, and simplicity of deposition even at room temperature.[2,3] Ga NPs can be tuned into the deep UV as a result of the high plasma frequency of Ga, ω_p = 14 eV, with demonstrated tunability over a broad spectral range from 0.75−6.5 eV, a significant advantage over the limited range achievable for either Ag or Au, especially for simultaneous UV Raman/photoluminescence (PL) spectroscopy.[2,4,5] Moreover, substrate-supported Ga NPs exhibit no postdeposition aggregation or attendant modification of the plasmon; therefore, the plasmon resonance is stable and reproducible. Unlike Ag and Au, Ga can be deposited directly onto solid supports, such as sapphire or Si, without an additional adhesion layer. Therefore, stable Ga NPs can potentially overcome the drawbacks associated with uncontrolled NP aggregation, yielding reproducibly tunable plasmonic substrates.

We have previously demonstrated that the Ga NP surface plasmon resonance (SPR) is minimally red-shifted and not quenched when exposed to air.[2] The Ga SPR remains stable and protected upon oxidation, even after over a year of air exposure. Conversely, Ag oxidizes excessively and becomes quenched within 36 h of air exposure.[6] In addition, the Ga plasmon mode's remarkable thermal stability from 80 K[7] to 873 K[2] foreshadows the advantageous use of Ga for applications in thermally harsh and diverse environments. Given these promising and unique attributes, we here demonstrate room-temperature-deposited, tunable, plasmonic Ga nanoparticles and their applicability to SERS.

The Raman enhancement and longevity of Ga NP substrates were tested using the standard Raman dye cresyl fast violet (CFV). Ga NPs were grown by molecular beam epitaxy on inert sapphire substrates to mitigate the fluorescence interference typically observed in Raman measurements with glass substrates, but they can be deposited on a wide variety of solid supports.[2] By adjusting the deposition time at a fixed beam flux, we modified the mean NP diameter and therefore tuned the SPRs of three Ga NP/sapphire substrates to (i) 2.9, (ii) 1.96, and (iii) 1.58 eV, as shown by the pseudoextinction coefficient, <*k*>, measured by in situ spectroscopic ellipsometry[2,8] (Figure 1).

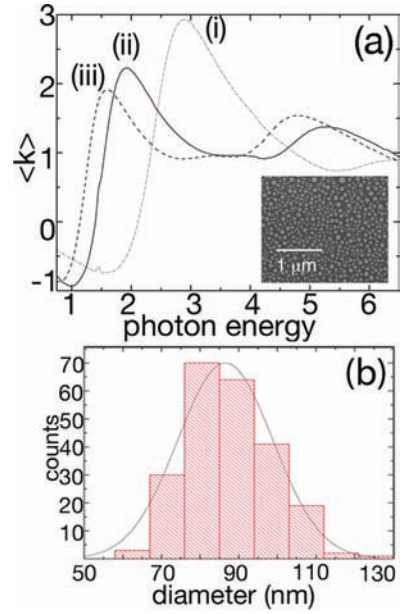

Figure 1. (a) Pseudoextinction spectra obtained by in situ spectroscopic ellipsometry corresponding to three Ga NP/sapphire samples. The SEM image (inset) and accompanying NP diameter distribution histogram (b) correspond to the 2.9 eV SPR sample [curve (i) in (a)].

The substrates were half metallized and half unmetallized for direct comparison of the Ga NPs' influence and the bare sapphire. A 1 μL volume of 100 ppm CFV in ethanol was dropwise placed on fully oxidized Ga NP/sapphire substrates and dried for ∼15 min to ensure complete EtOH evaporation and minimize the distance between the CFV molecules and the metal NP surfaces. CFV and sapphire possess distinct, strong, and well-separated Raman-active modes. EtOH easily wets the substrate surface, and the solution spreads over a circular area of ∼5 mm × 5 mm = 25 mm^2.

The strong Raman-active CFV mode at 590 cm^{-1} was measured using a Renishaw inVia Raman system with a 50× objective (∼2 μm diameter beamspot) and a 0.2 mW 633 nm HeNe laser. A 100 ppm solution of CFV in EtOH was deposited on both the metallized and bare halves of each sample. The aggregate Raman enhancement for a given sample is simply given by R/f_{NP}, where $R = I_{NP}/I_{bare}$ is the ratio of the two Raman measurements (averaged over five different locations) and f_{NP} is the fraction of the surface area covered by nanoparticles in the SEM image. The clear difference with and without Ga NPs on the surface indicates that the nanostructured

† Department of Electrical and Computer Engineering, Duke University.
‡ Department of Biomedical Engineering, Duke University.
§ Department of Physics, Duke University.
|| Institute for Inorganic Methodologies and of Plasmas.
⊥ Army Aviation and Missile RD&E Center.

10.1021/ja903321z CCC: $40.75

Ga induces an enhancement of the Raman signal (Figure 2). The 2.9 eV SPR sample exhibited the strongest aggregate SERS enhancement (~30/0.37 = 80), followed by the 1.58 eV and 1.96 eV samples. Although we did not attempt to discern the enhancement factor,[9,10] an unknown fraction of the heterogeneously distributed particle sizes and spacings enhanced the Raman signal, and it is clear that the enhancement factor will be orders of magnitude larger when the few regions responsible for the enhancement are identified.

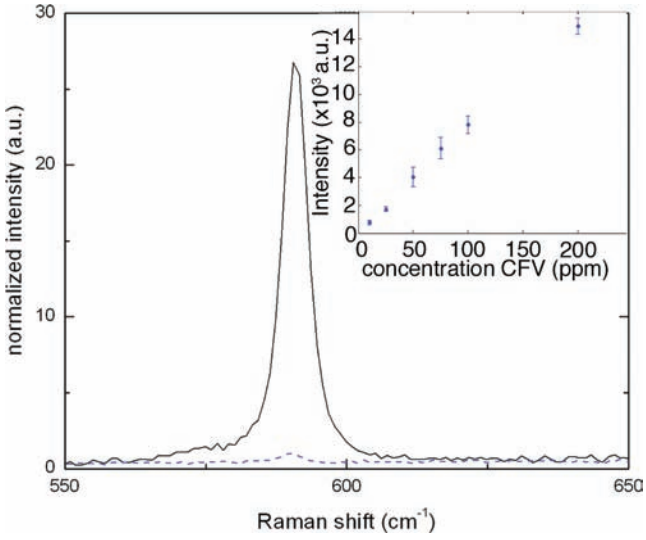

Figure 2. High-resolution Raman spectrum for the strongest CFV mode at 590 cm^{-1} for Ga NPs with the SPR at 2.9 eV (solid) compared with that for the same CFV mode on bare sapphire (dashed). Inset: linear correlation between CFV concentration and Raman intensity revealed by varying the CFV concentration in the deposition solution. The calibration error bars, determined as the standard deviation for five measurement locations, were quite small (4−20%), even at the largest concentrations, indicating reproducibility.

To quantify the sensitivity and postoxidation stability of the enhanced Raman signal from the 2.9 eV NPs, CFV solutions with concentrations ranging from 10−200 ppm were deposited onto the Ga NPs on sapphire for Raman measurements (Figure 2, inset). As expected, the Raman intensity decreased linearly with decreasing CFV concentration, but even the 10 ppm sample exhibited a measurable Raman signal. In stark contrast to Ag nanostructures used for SERS substrates, the Ga NP-enhanced Raman signal did not degrade even after several days of air exposure.

Several factors contribute to the varying enhancements among the three plasmonic Ga NP/sapphire substrates. Enhanced Raman signals arise from strong localized surface modes of plasmonic NPs. Since all of the Ga NPs were spheroidal, the plasmon resonance of these samples were tuned with NP size. Inspection of the Ga NP imagery supports a correlation between NP size and enhanced Raman signal: the 2.9 eV sample, whose NPs had the smallest mean diameter (88 nm), contributed the strongest Raman response. In addition, the high density of NPs associated with the smallest mean diameter increases the opportunity for interparticle electromagnetic coupling and field concentration between the NPs. The interparticle spacings in the 2.9 eV sample were most narrowly distributed around a mean separation of 16 nm, which is small enough to induce strong interparticle electric-field coupling to enhance the local fields, ultimately strengthening the already enhanced Raman signal.[11] As the NPs increase in size, so does the interparticle spacing (20 nm for the 1.96 eV substrate and 40 nm for the 1.58 eV substrate), weakening any enhancement derived from interparticle electromagnetic coupling. Taken together, the large number of small, similarly sized, closely spaced NPs enables the 2.9 eV sample to produce the strongest Raman signal for a given concentration of CFV. Importantly, tuning the Ga NP diameter and spacing during growth can optimize the NP-induced enhancement.

Plasmonic Ga NPs can be flexibly applied to a variety of applications because of their tunability over a broad spectral range, liquid phase, and attendant thermal and chemical stability. In a self-assembled, room-temperature, UHV evaporation process, Ga NPs are tunable to specific plasmon resonances ranging from 0.75 to 6.5 eV. Although the enhancement factor for these Ga NPs is smaller than reported for Ag nanostructures, it is important to emphasize that enhanced Raman signals were observed even though the room-temperature deposition produced nonoptimized NP density and size distributions. The tremendous control afforded by MBE deposition and Ostwald ripening to tailor the Ga NP distribution, with more uniformly sized NPs or more controllable NP densities, heralds the potential of reproducibly self-assembled plasmonic Ga NPs for SERS.

Acknowledgment. This work was partially supported by the U.S. Army's competitive in-house innovative research program and the National Institutes of Health (R01 EB006201). The authors thank Jon Scaffidi for helpful discussions. H.O.E. thanks R. Van Duyne for his supportive comments during the early phases of this project.

References

(1) Zeman, E. J.; Schatz, G. C. *J. Phys. Chem.* **1987**, *91*, 634–643.
(2) Wu, P. C.; Kim, T.-H.; Brown, A. S.; Losurdo, M.; Bruno, G.; Everitt, H. O. *Appl. Phys. Lett.* **2007**, *90*, 103119.
(3) Wu, P. C.; Losurdo, M.; Kim, T.-H.; Choi, S.; Bruno, G.; Brown, A. S. *J. Vac. Sci. Technol., B* **2007**, *25*, 1019–1023.
(4) Haes, A. J.; Haynes, C. L.; McFarland, A. D.; Schatz, G. C.; Van Duyne, R. P.; Zou, S. *MRS Bull.* **2005**, *30*, 368–375.
(5) Quinten, M. *Z. Phys. B* **1996**, *101*, 211–217.
(6) McMahon, M.; Lopez, R.; Meyer, H.; Feldman, L.; Haglund, R. *Appl. Phys. B: Lasers Opt.* **2005**, *80*, 915–921.
(7) Parravicini, G. B.; Stella, A.; Ghigna, P.; Spinolo, G.; Migliori, A.; d'Acapito, F.; Kofman, R. *Appl. Phys. Lett.* **2006**, *89*, 033123.
(8) Oates, T. W. H.; Mucklich, A. *Nanotechnology* **2005**, *16*, 2606–2611.
(9) Haynes, C. L.; Van Duyne, R. P. *J. Phys. Chem. B* **2003**, *107*, 7426–7433.
(10) Jackson, J. B.; Halas, N. J. *Proc. Natl. Acad. Sci. U.S.A.* **2004**, *101*, 17930–17935.
(11) Gunnarsson, L.; Bjerneld, E. J.; Xu, H.; Petronis, S.; Kasemo, B.; Kall, M. *Appl. Phys. Lett.* **2001**, *78*, 802–804.

JA903321Z